Electro-Optic Crosstalk in Parallel Silicon Photonic Mach-Zehnder Modulators

Lingjun Jiang, Xi Chen, Kwangwoong Kim, Guilhem de Valicourt, Zhaoran Rena Huang and Po Dong

***Abstract*—Dense integration of electro-optic (EO) devices in photonic integrated circuits (PICs) is critical to achieve high-capacity, compact and low-cost transceiver modules and fulfill the increasing bandwidth and/or bandwidth density demands for future computers, severs, data centers, and transport optical network systems. However, the EO crosstalk due to high integration density may degrade the transmission performance and eventually limit the possible density of integration. In this content, the study of the EO crosstalk of a PIC and its impact is crucial. In this paper, we systematically investigate and characterize the EO crosstalk between parallel silicon Mach-Zehnder modulators (MZMs). The performance penalty due to crosstalk is measured for different integration densities and data rates. For the MZM pair with a separation of 200 μm, there is a ~ -20 dB RF crosstalk in the frequency range >10 GHz, and up to 1.1 dB power penalty and 2.2 dB optical signal-to-noise ratio (OSNR) penalty are observed for 36-Gb/s on-off-keying (OOK) signals. Our study can serve as a reference for integration density of large-scale silicon PICs for various applications.**

***Index Terms*—Modulator, Integrated optics, Electro-optic crosstalk**

I. Introduction

With the fast growth of date volume in the information age, the data transmission rate, whether in long-distance communication systems or chip-scale microprocessors, has been immensely increasing. To keep up with the trend and support high-speed applications such as board-to-board and chip-to-chip optical interconnect, photonic systems are expected to handle more efficient data transmission while remaining compact and energy efficient. There are several approaches having been developed to address this challenge. For example, wavelength-division multiplexing (WDM) has been realized by utilizing on-chip arrayed waveguide gratings (AWGs) [1] or cascaded Mach-Zehnder interferometers (MZI) [2, 3], and polarization-division multiplexing (PDM) modulation is also demonstrated for EO quadrature phase-shift keying (QPSK) modulators [4]. All these approaches to increase the bandwidth and/or bandwidth density require dense integration implemented in PICs.

Dense optical integration is one of the most important advantages of silicon photonics technology [5]. Compared with other PICs based on silica, polymers, and III-V materials, silicon photonics is expected to achieve both compactness and efficiency by integrating a number of devices on a single chip enabled by modern CMOS processing. Over the past decade, vast progress has been made in developing integrated on-chip photonic devices like lasers [6], low-loss waveguides [7, 8], high-speed modulators [9, 10], photodetectors [11-13], etc. Various optical transceiver modules based on silicon photonic technology have also been developed [14, 15], indicating tremendous potential and opportunities offered by this technology.

However, dense photonic integration will cause crosstalk among channels at high data rates. In particular for active devices, dense integration may introduce severe RF crosstalk since RF wavelengths are much longer than optical wavelengths [16]. While the optical wave is tightly confined in optical waveguides, its electrical counterpart may affect neighboring devices by mutual inductance and capacitance coupling [17], or RF radiations.

There were a few preliminary research efforts recently to investigate and address this crosstalk issue. Work has been done to solve the crosstalk issue in a transmitter optical sub-assembly (TOSA) [18], which is able to operate at 100 Gb/s with almost no crosstalk penalty. While [18] mainly focuses on electrical design to reduce crosstalk in the RF boards, Ref. [19] characterizes the crosstalk issues in III-V PICs. A digital pre-compensation scheme is also demonstrated for quadrature amplitude modulation (QAM) signals in in-phase/quadrature (I/Q) modulators [20], where Q^2 factor is improved by 4.4 dB and 64-QAM performance is improved significantly.

In this paper, we focus on the study of the EO crosstalk between two neighboring silicon MZMs with OOK signals and experimentally characterize the impact of crosstalk on bit-error ratio (BER) at different data rates. Similarly, crosstalk-induced power penalty has been presented in Indium Phosphide (InP) MZM structure in [19]. However, a >15 dB power penalty at the data rate of 10 Gb/s at 10^{-5} BER has been found with a crosstalk level of ~-21 dB in [19]. Our key result shows that with similar EO crosstalk level, the penalty is only about 1.1 dB at 36 Gb/s at a BER of 10^{-8}. We also performed system level numerical simulation to verify that our experimental results are reasonably comparable to the simulation results.

Manuscript received May, 2017; revised October, 2017; accepted December, 2017.

Lingjun Jiang was with Bell Laboratories, Nokia, 791 Holmdel Road, Holmdel, NJ 07733, USA. She is now with Department of Electrical, Computer and Systems Engineering, Rensselaer Polytechnic Institute, 110 8th Street, Troy, NY 12180 USA (email: jiangl2@rpi.edu).

Zhaoran Rena Huang is with Department of Electrical, Computer and Systems Engineering, Rensselaer Polytechnic Institute, 110 8th Street, Troy, NY 12180 USA (email: zrhuang@ecse.rpi.edu).

Other authors are with Bell Laboratories, Nokia, 791 Holmdel Road, Holmdel, NJ 07733, USA (email: xi.v.chen@nokia-bell-labs.com; kw.kim@nokia-bell-labs.com; guilhem.de_valicourt@nokia-bell-labs.com; po.dong@nokia-bell-labs.com).

This article has been accepted for publication in a future issue of this journal, but has not been fully edited. Content may change prior to final publication. Citation information: DOI 10.1109/JLT.2018.2789582, Journal of Lightwave Technology

The paper is organized as follows. First, we present the simulated RF coupling between the MZMs and explored its impact on BER penalty for the OOK modulation through modeling. Next, we describe the test structure and discuss our experimental results. The measurements include the frequency response of the EO crosstalk, optical power penalty and OSNR penalty. Our systematic characterization may be used as a guideline for the design of highly integrated transceivers for optical interconnect and communication systems.

II. Theoretical Study of Electro-Optic Crosstalk

The EO crosstalk in MZMs originates from the RF coupling between traveling-wave electrodes of the modulators. The state-of-the-art depletion-type silicon MZMs based on the use of PN junctions are usually several millimeters long. To ensure impedance match and reduce microwave attenuation, coplanar waveguide or slotline traveling-wave electrodes have been widely used [21-23]. While optical wave is very well confined in the single-mode waveguides, the high frequency electrical signal could couple between two transmission lines through mutual inductance and capacitance, as illustrated in Fig. 1. In this section we analyze the EO crosstalk and the BER in order to investigate the magnitude of the RF coupling from the neighboring modulator and the degree of degradation of BER due to the crosstalk.

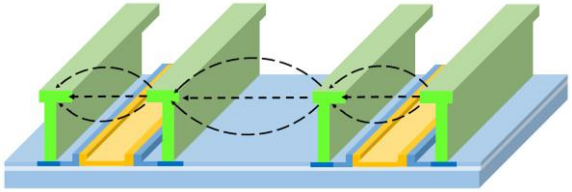

Fig. 1. Schematic of RF crosstalk between MZMs that have slotline traveling wave electrodes.

A. Simulation of S parameters

We first studied RF coupling by calculating S parameters of the traveling-wave electrodes of the MZMs. Commercial software package Advanced Design System (ADS) is used to build the circuit model for analysis. As illustrated in Fig. 2, two identical transmission lines, separated by a distance of D, are in parallel, each of which represents one MZM. Each MZM has one ground line and one signal line, separated by a distance of d. Port 1, 2 and port 3, 4 are used for the two MZMs, respectively, and the transmission lines are each terminated by a Z_0 = 50 Ω resistor. The series resistance and junction capacitance of the PN junction is denoted by R_0 and C_0, respectively, and chosen based on typical depletion-type MZM parameters. The total length of the MZM, L, is divided into a series of identical unit cells with 100 μm in length, while R_0 and C_0 are distributed for each unit cell in order to model the traveling wave. The RF signals are added to port 1, and received at port 2, so S_{21} represents the signal forward gain of the first MZM. Due to RF coupling, part of the electromagnetic wave couples to the second MZM and propagates towards port 4. The amplitude of the RF crosstalk can be measured by the ratio of S_{41}/S_{21}, indicating the portion of the voltage received at the MZM2 compared with MZM1.

Fig. 3 (a) shows the frequency response of the RF crosstalk between two MZMs for different D of 200 μm, 400 μm, 600 μm and 800 μm for L = 4 mm. Fig. 3 (b) shows the crosstalk for different device lengths L = 3 mm, 4 mm or 5 mm for D = 200 μm. Other parameters are chosen as C_0 = 0.02 pF/100 μm, R_0 = 10 Ω/100 μm, d = 90 μm, and the lines are aluminum of 2 μm thick with layer information of SOI wafer included.

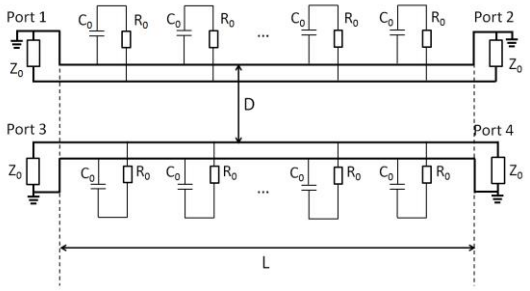

Fig. 2. Illustration of the circuit model of MZMs for S parameter simulation.

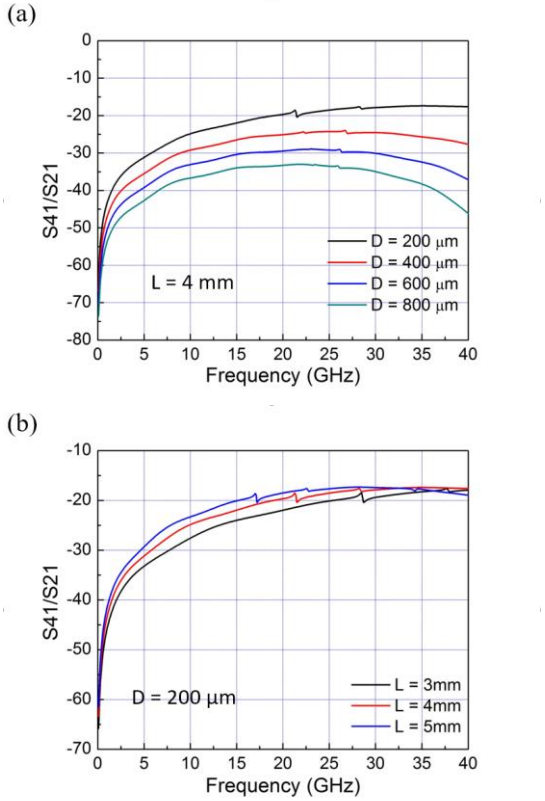

Fig. 3. Frequency response of RF crosstalk for (a) different separation D between MZMs, and (b) different MZM lengths.

The results shown in Fig. 3 demonstrated that the crosstalk increases with smaller D as expected since it originates from the coupling between two transmission lines. Due to the parasitic capacitance between the transmission lines, capacitive coupling is the main reason for crosstalk. It is very small at low frequencies, and increases to a maximum value determined by D, as shown in the plot. For the nearest MZM pair (D = 200 μm), the maximum RF crosstalk is -17.4 dB at f = 34 GHz. We notice that the frequency dependent crosstalk behavior (very small at low frequency and peak at certain frequency) is similar to those in InP MZMs, reported in [19], with a quasi-periodic dependence on the operating frequency accounting for the reduced crosstalk at high frequencies.

This article has been accepted for publication in a future issue of this journal, but has not been fully edited. Content may change prior to final publication. Citation information: DOI 10.1109/JLT.2018.2789582, Journal of Lightwave Technology

B. Theoretical simulation of BER penalty

A theoretical study of the relationship between the RF crosstalk and the BER penalty is needed to understand the impact of the crosstalk on modulator performance. RF coupling does not necessarily make a substantial difference for the operation of the MZMs in terms of EO modulation, since there always exist system noise and other distortions that already impact the MZMs to some degree. For certain modulation scheme, the performance of the MZMs can be characterized by the BER penalty. The RF crosstalk becomes an issue only if the BER of the MZM increases by a visible amount.

To quantitatively estimate the BER penalty due to RF crosstalk, numerical simulations are carried out. The simulated system is a 25-Gb/s OOK intensity modulated and direct detection (IM-DD) system. At the transmitter, two independent pseudorandom binary sequence signals (PRBS), S_0 and S_{xt}, are generated. The S_0 and S_{xt} are respectively the signal and the crosstalk. Assuming the crosstalk level is β (normalized to signal power), the received signal with crosstalk is

$$S' = S_0 + \sqrt{\beta}\, S_{xt}. \qquad (1)$$

This crosstalk level β in Eq. (1), is defined as the ratio between the signal power and the crosstalk power. After adding crosstalk, white Gaussian noise is added to emulate different received OSNR levels. The signal is received by a photodiode. To simplify the simulation, here the photodiode is assumed to have no bandwidth limitation and no additional noises. At last, symbol decisions are made with optimized decision thresholds. For each OSNR level, the simulated pattern length is $2^{21} - 1$, and the simulation is done 10,000 times to achieve a total simulated number of bits of 2.1×10^{10}. In this way, BER level lower than 1×10^{-9} can be counted. Every repeat simulation uses randomly generated S_0, S_{xt}, and random white Gaussian noises.

Since the purpose of this simulation is to obtain a general idea of the crosstalk impact on OOK signals, no frequency dependence is considered for β. In other words, β is a constant value for all frequencies. Practical crosstalk levels vary over frequencies, which will be measured and studied in Section IV. Also, as we'd like to study how much degradation the crosstalk itself can cause, other components (modulator, photodiode, etc.) are considered to be ideal.

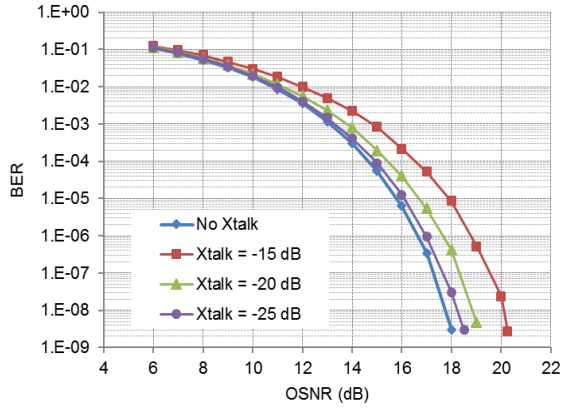

Fig. 4. BER vs OSNR curves for different levels of RF crosstalk. Here the crosstalk levels are the same for all the frequencies.

Fig. 4 shows the simulated BERs as a function of OSNR for various crosstalk levels. It can be seen that the OSNR penalty is larger at lower BER levels. For example, for the crosstalk level of -15 dB, the penalty can be 1.5 dB if BER is 1×10^{-3} and 2.1 dB if it is 1×10^{-8}. This is understandable, as the RF crosstalk affects BER significantly only if it is comparable to or dominates over other noise/distortion contributions. We use -25 dB, -20 dB and -15 dB crosstalk to simulate different crosstalk levels. In reality, the crosstalk level can be determined by various factors, e.g. spacing between the MZMs, and/or RF power ratio of the aggressor MZM and the signal MZM's. From the result, at BER = 1×10^{-8}, the OSNR penalty for the crosstalk level of -25 dB, -20 dB and -15 dB are 0.5 dB, 1 dB and 2.4 dB, respectively. We'd like to address again that the results in Fig. 4 use a simple model which assumes constant crosstalk over frequencies. This is sufficient for understanding the crosstalk impact on OOK signals. Modeling the real crosstalk in a particular chip is case-by-case so much more complicated and is out of the scope of this simulation.

III. Device Design

To experimentally characterize the EO crosstalk and its impact on the BERs, we designed an array of parallel MZMs, numbered from 1 to 8, as shown in Fig. 5 (a). There are four pairs of MZMs, and each pair of MZMs has one signal MZM for modulation, and one aggressor MZM to generate crosstalk, as shown in Fig. 5 (b). They are fabricated on a SOI substrate with 220 nm Si layer and 3 μm box layer. In order to study how the integration density affects the crosstalk, the signal and aggressor MZMs are separated by D1 = 200 μm, D2 = 400 μm, D3 = 600 μm and D4 = 800 μm, respectively. The MZMs have phase shifters of 3 mm long, and are driven by push-pull configurations. Traveling-wave electrodes are used to apply high speed RF signals, with the signal line and the ground line separated by 30 μm. At the end of the electrodes, a ~45 Ω termination resistor is used. The MZMs have a V_π of ~6 V, and other detailed device information can be found in [24].

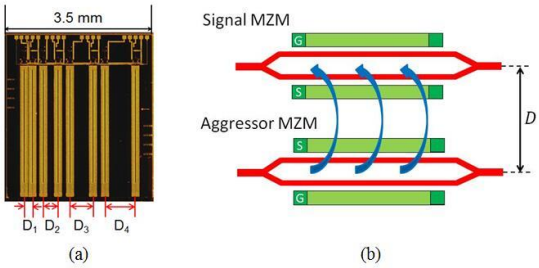

Fig. 5. (a) Optical micrograph of the MZMs. (b) Top view schematic of the MZM pair for crosstalk measurement.

IV. Experimental Results

The performance of an MZM can be represented by BER under certain modulation scheme. Due to EO crosstalk, extra optical power or OSNR may be required by the system to achieve the same BER level. Therefore the crosstalk effect can be characterized by power penalty and OSNR penalty, which are experimentally measured and presented in this section. For simplicity we use OOK modulation format for all measurements.

A. Frequency Response of Electro-optic Crosstalk

The frequency response of the EO crosstalk is measured for the first pair of MZMs (1 and 2) with a lightwave component

This article has been accepted for publication in a future issue of this journal, but has not been fully edited. Content may change prior to final publication. Citation information: DOI 10.1109/JLT.2018.2789582, Journal of Lightwave Technology

analyzer (LCA) which covers the frequency range of 100 MHz to 20 GHz. The MZMs are biased at quadrature, and the RF drive signal power from the LCA is 5 dBm. MZM1's own EO response is taken and plotted in Fig. 6 (a), which shows a 3 dB bandwidth of over 20 GHz. The signals are then applied to the input port of MZM2, while the optical response is taken at the output port of MZM1. The measured crosstalk is then normalized to the MZM1's EO response, and plotted in Fig. 6 (b). It shows that the crosstalk increases with frequency and remains at about -20 dB when the frequency is above 8 GHz. This result is very close to the simulation result in Fig. 3 (b), where the RF crosstalk is around -20 dB at the frequency of 20 GHz. As crosstalk increases with frequency, it will degrade the modulation with higher data rates which have more high frequency components.

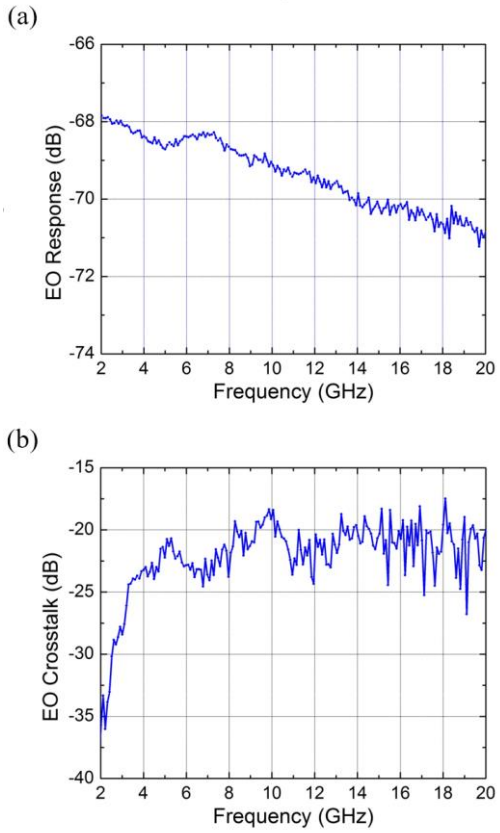

Fig. 6. (a) EO response of MZM1. (b) EO crosstalk between MZM 1 and 2.

B. Experimental Setup and Eye Diagram

The performance penalty due to EO crosstalk is characterized by BER measurement. We use direct detection scheme, and the experimental setup is shown in Fig. 7. The equipment labeled in green and pink denote electrical and optical paths, respectively. A pattern generator is used to provide two streams of PRBS of identical power, which are amplified and applied to the MZMs. In this experiment we apply the same RF power into MZM1 and MZM2. We add a delay between the two signals by using electrical cables of different lengths, in order to mimic crosstalk noises from MZM2 to MZM1. Two high-speed ground-signal (GS) RF probes are used to feed the signals, and we arrange the probes in a GSSG manner, which generates maximum possible crosstalk [20]. A tunable laser provides the optical source of λ = 1532 nm, and the polarization controller is tuned to obtain maximum optical output power. We use two optical attenuators in the setup to measure BER from different aspects. The one after the MZMs is used to change OSNR, and the one before the receiver is to control the received optical power. The optical receiver is capable of detecting 40 Gb/s OOK signal with a 3-dB bandwidth in the range of 25-30 GHz. After passing the receiver and the 4:1 demultiplexer, the signals are sent to a 12.5 Gb/s error detector which measures the BER. A synthesizer is used to provide a common clock that controls the pattern generator, the demultiplexer and the error detector.

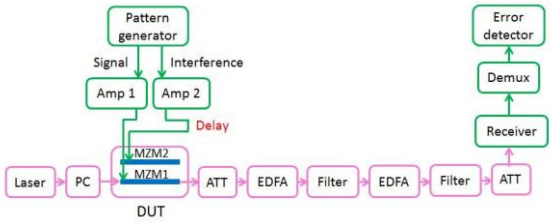

Fig. 7. Experiment setup. PC: polarization controller, DUT: device under test, ATT: attenuator, EDFA: Erbium-doped fiber amplifier.

The drive voltage is 5 V for both MZMs. Eye diagrams are taken at 10 Gb/s, 25 Gb/s and 36 Gb/s, at two different OSNR levels of 20 dB and 30 dB, as shown in Fig. 8.

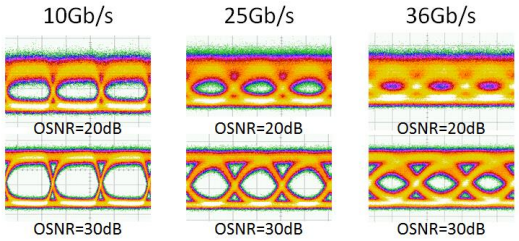

Fig. 8. Eye diagrams of the tested silicon modulator at 10 Gb/s, 25 Gb/s and 36 Gb/s.

C. Power penalty

Power penalty is calculated by measuring the BER as a function of received optical power, while keeping OSNR at a fixed level. For each MZM pair, BER versus optical power curve is first measured for the signal MZM, when the aggressor MZM does not carry any RF signal, and the result is compared with the case when the aggressor MZM's driving signals are simultaneously turned on.

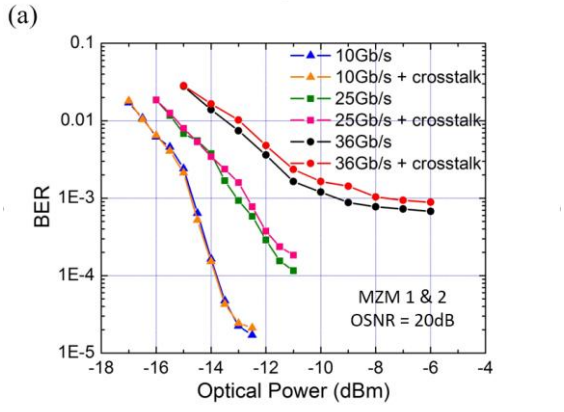

This article has been accepted for publication in a future issue of this journal, but has not been fully edited. Content may change prior to final publication. Citation information: DOI 10.1109/JLT.2018.2789582, Journal of Lightwave Technology

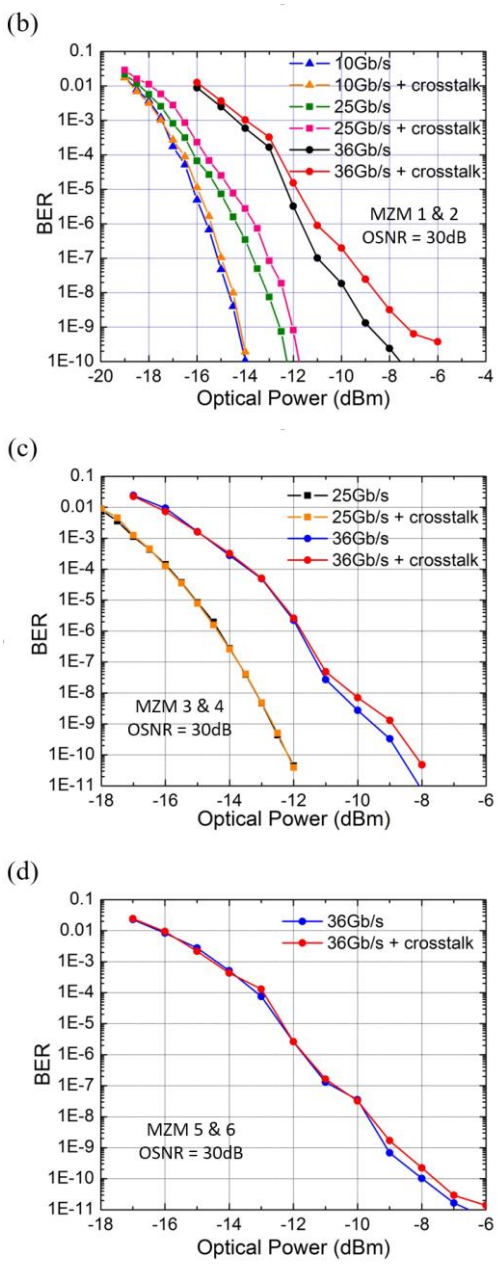

Fig. 9. BER vs optical power for (a) MZM 1 and 2 at OSNR=20 dB, (b) MZM 1 and 2 at OSNR=30 dB, (c) MZM 3 and 4 at OSNR=30 dB, and (d) MZM 5 and 6 at OSNR=30 dB.

The results are plotted in Fig. 9. Figs. 9 (a) and (b) are for MZM 1 and 2 (D1=200 μm), with an OSNR of 20 dB and 30 dB, respectively. When OSNR is 20 dB, BER is greater than 10^{-5}. In this case the EO crosstalk does not significantly affect the BER, since other optical noise [mainly amplified spontaneous emission (ASE) noises from EDFA] dominates, as implied by the eye diagram in Fig. 8. At 10 Gb/s, the power penalty is negligible, and increases by only a small amount when the data rate goes up. When OSNR is 30 dB, the influence of RF crosstalk starts to show up, as shown in Fig. 9 (b). Under such low ASE noise, BER can almost reach zero given enough optical power. It can be seen that BER can only be observed at low BER. The RF crosstalk does not make a difference when the optical power is small and BER is high, whereas the receiver noise dominates. To keep consistency with the modeling results in Section II, we compare the penalty when BER equals $1x10^{-8}$ for all the measurements in this section. Although $1x10^{-8}$ BER is not used in real communication systems, we chose this value to achieve appreciable power penalty and a reasonable comparison with the simulation in Section II. It is observed that the power penalty at BER = $1x10^{-8}$ is negligible at 10 Gb/s, increases to 0.5 dB at 25 Gb/s and eventually reaches ~1.1 dB at 36 Gb/s, in consistency with our frequency response results.

Since we did not see obvious power penalty at OSNR = 20 dB, the BER vs power curves for MZM 3, 4 and 5, 6 are only plotted for OSNR = 30 dB. For MZM 3 and 4 (D2 = 400 μm), there is no penalty at 25 Gb/s, and at 36 Gb/s the power penalty is 0.4 dB at BER = $1x10^{-8}$, as shown in Fig. 9 (c). The third pair MZM 5 and 6 (D3 = 600 μm) is only measured at 36 Gb/s, and the power penalty is negligible, as shown in Fig. 9 (d). Fig. 10 summarizes the power penalty measurement.

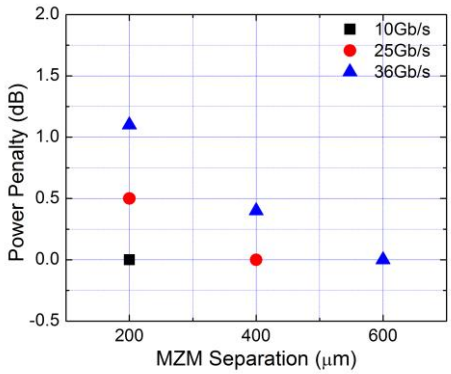

Fig. 10. Crosstalk-induced power penalty at BER = $1x10^{-8}$ for 3 data rates.

D. OSNR penalty

We also measured the OSNR sensitivity of the crosstalk effect, while keeping the received optical power fixed. It is clear that OSNR penalty acts in the same manner as power penalty: it increases with data rate, and decreases with MZM separation. For consistency, the received optical power is chosen as the same value as in the power penalty measurement for certain OSNR levels. For simplicity, we only plotted in Fig. 11 part of the results that are enough to show the trend of OSNR penalty. For MZM 1 & 2, as shown in Fig. 11 (a), the penalty is negligible at BER = $1x10^{-8}$ at 10 Gb/s with -14 dBm optical power. It becomes 1.5 dB at 25 Gb/s with -12 dBm optical power (Fig. 11 (b)), and increases to 2.2 dB at 36 Gb/s with -8 dBm optical power (Fig. 11 (c)), corresponding to stronger RF coupling at higher frequencies. For the second pair MZM 3 & 4, the penalty is negligible at 25 Gb/s with -12 dBm optical power, and increases to 1.7 dB at 36 Gb/s with -8 dBm optical power, as shown in Fig. 11 (d) and (e). For the third pair MZM 5 & 6, the penalty is negligible even at 36 Gb/s with -8 dBm optical power, as shown in Fig. 11 (f), which is consistent with the optical power penalty measurement in Part C. The OSNR penalty results are summarized in Fig. 12.

This article has been accepted for publication in a future issue of this journal, but has not been fully edited. Content may change prior to final publication. Citation information: DOI 10.1109/JLT.2018.2789582, Journal of Lightwave Technology

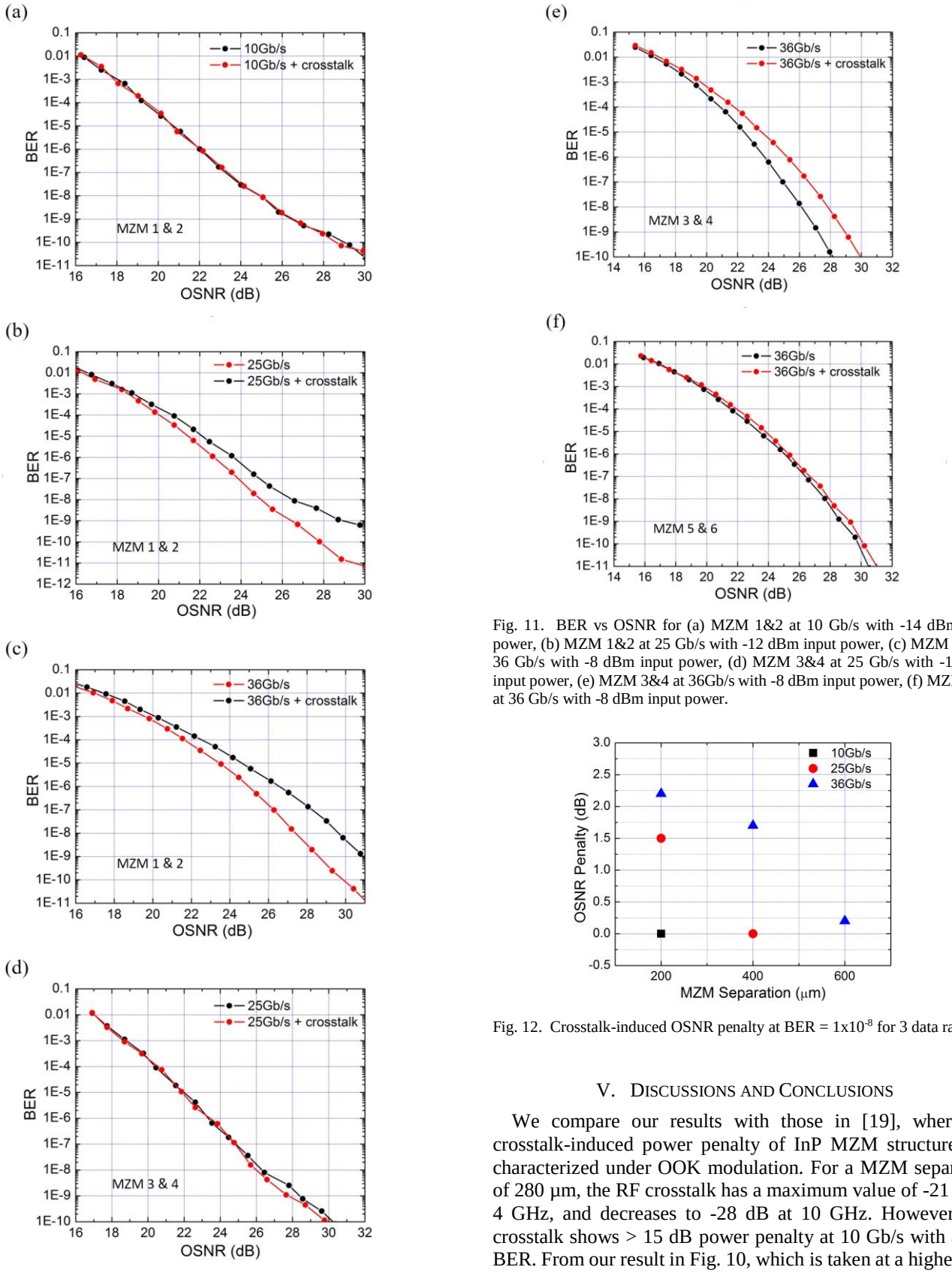

Fig. 11. BER vs OSNR for (a) MZM 1&2 at 10 Gb/s with -14 dBm input power, (b) MZM 1&2 at 25 Gb/s with -12 dBm input power, (c) MZM 1&2 at 36 Gb/s with -8 dBm input power, (d) MZM 3&4 at 25 Gb/s with -12 dBm input power, (e) MZM 3&4 at 36Gb/s with -8 dBm input power, (f) MZM 5&6 at 36 Gb/s with -8 dBm input power.

Fig. 12. Crosstalk-induced OSNR penalty at BER = $1x10^{-8}$ for 3 data rates.

V. Discussions and Conclusions

We compare our results with those in [19], where the crosstalk-induced power penalty of InP MZM structure was characterized under OOK modulation. For a MZM separation of 280 μm, the RF crosstalk has a maximum value of -21 dB at 4 GHz, and decreases to -28 dB at 10 GHz. However, this crosstalk shows > 15 dB power penalty at 10 Gb/s with a 10^{-5} BER. From our result in Fig. 10, which is taken at a higher data rate and a lower BER, the MZM pair with a separation of 200 μm only has a maximum of 1.1 dB power penalty. Even after considering possible different OSNR levels, this enormous disagreement still cannot be explained. Since we have seen

greater consistency of the power penalty and OSNR penalty with our numerically simulated BER curves in Fig. 4, it's reasonable to say that our measurement gives a better reference of the penalties. One possible explanation of the results in [19] may be the underestimated crosstalk in InP MZMs.

Since the EO crosstalk acts as distortion to degrade signal quality, same crosstalk shall introduce same power penalty, as modeled in Section II. Therefore, the measured results shall be applicable to modulators with similar crosstalk under OOK modulation. However, it's worth noting that we have made a few assumptions in our study. First, the RF powers into the signal channel and the aggressor channel are the same, while in real systems this may not be exactly true. Different RF power ratios between the aggressor channel and signal channel will result in different crosstalk levels, which is not experimentally measured in this paper. However, once the actual crosstalk level is determined, one can always use our measured or simulated 'xtalk level vs. OSNR penalty' as reference numbers. Secondly, we assume the MZMs are working in the linear region, but if the input large RF drive signal operates in the nonlinear regime of the MZM, the EO-crosstalk induced power penalty will be dependent on the input RF power. Thirdly, the RF coupling between transmission lines relies on the electrode and silicon design of the modulator. Although this work is focused on crosstalk characterization and its penalty, it's desirable to reduce crosstalk from the modulator design point of view. However, dense integration in PICs would be always preferable in future applications and thus the electro-optic crosstalk is inevitable. Therefore, it is still critical to investigate the crosstalk and its impact, as presented in this paper.

Since the RF crosstalk between two MZMs is partly deterministic, it opens a potential for compensation. Nevertheless, the compensation requires the phase information of the crosstalk as well as amplitude and this may require coherent detection of the modulated fields, as shown in [20]. For IM/DD systems, as the phase of the signal is not detected, the compensation may be challenging.

In conclusion, we theoretically studied the RF coupling between parallel MZMs and numerically related the magnitude of RF crosstalk to BER penalty. Then we experimentally characterized the EO crosstalk between two silicon MZMs separated by a distance of 200 μm, 400 μm and 600 μm. By measuring BERs under OOK modulation, it is found that the impact of crosstalk decreases with MZM separations and increases with data rate. For the closest MZM pair with a separation of 200 μm, 1.1 dB power penalty and 2.2 dB OSNR penalty are observed at 36 Gb/s at BER level of $1x10^{-8}$ with an EO crosstalk level of ~-20 dB at >10 GHz. This result raises a challenge in dense integration of photonic circuits, which may require better packaging techniques and compensation schemes. Our study also provides a guideline to the trade-off between system integration and performance optimization.

ACKNOWLEDGMENT

We thank Tsung-Yang Liow and Guo-Qiang Lo of the Institute of Microelectronics, Singapore on fabrication, Jeffrey Sinsky for helpful discussions on microwave simulations, and Young-Kai Chen, Peter Winzer and Sethumadhavan Chandrasekhar for their support. This work was partly supported by an Institute for Information & Communications Technology Promotion grant from the Korean government (MSIP), B0101-16-0021, "Development of key technologies for flexible optical nodes in software-defined network".

REFERENCES

[1] D. Dai *et al*., "Design and fabrication of ultra-small overlapped AWG demultiplexer based on-Si nanowire waveguides," *Electron. Lett.*, vol. 42, no. 7, pp: 400-402, 2006.

[2] A. Liu *et al*., "Wavelength division multiplexing based photonic integrated circuits on silicon-on-insulator platform," *IEEE J. Sel. Topics Quantum Electron.*, vol. 16, no. 1, pp: 23-32, 2010.

[3] F. Horst *et al*., "Cascaded Mach-Zehnder wavelength filters in silicon photonics for low loss and flat pass-band WDM (de-) multiplexing," *Opt. Express*, vol. 21, no. 10, pp: 11652-11658, 2013.

[4] P. Dong, *et al*., "112-Gb/s monolithic PDM-QPSK modulator in silicon," *Opt. Express*, vol. 20, no. 26, pp: B624-B629, 2012.

[5] A. Alduino *et al*., "Interconnects: wiring electronics with light," *Nature Photon*., vol. 1, no. 3, pp: 153-155, 1997.

[6] M. Pollnau *et al*., "Double tungstate lasers: From bulk toward on-chip integrated waveguide devices," *IEEE J. Sel. Topics Quantum Electron.*, vol. 13, no. 3, pp: 661-671, 2007.

[7] K. K. Lee *et al*., "Fabrication of ultralow-loss Si/SiO_2 waveguides by roughness reduction," *Opt. Lett.*, vol. 26, no. 23, pp: 1888-1890, 2001.

[8] Vlasov, Yurii, and Sharee McNab. "Losses in single-mode silicon-on-insulator strip waveguides and bends," *Opt. Express*, vol. 12, no. 8, pp: 1622-1631, 2004.

[9] Q. Xu *et al*., "Micrometre-scale silicon electro-optic modulator," *Nature*, vol. 435, no. 7040, pp: 325-327, 2005.

[10] P. Dong *et al*., "Low V pp, ultralow-energy, compact, high-speed silicon electro-optic modulator," *Opt. Express*, vol. 17, no. 25, pp: 22484-22490, 2009.

[11] L. Vivien *et al*., "42 GHz pin Germanium photodetector integrated in a silicon-on-insulator waveguide," *Opt. Express*, vol. 17, no. 8, pp: 6252-6257, 2009.

[12] D. Feng *et al*., "High-speed Ge photodetector monolithically integrated with large cross-section silicon-on-insulator waveguide," *Appl. Phys. Lett*., vol. 95 no. 26, pp: 261105, 2009.

[13] X. Gan, *et al*., "Chip-integrated ultrafast graphene photodetector with high responsivity," *Nature Photon*., vol. 7, no. 11, pp: 883-887, 2013.

[14] C. Li *et al*., "A ring-resonator-based silicon photonics transceiver with bias-based wavelength stabilization and adaptive-power-sensitivity receiver," *IEEE International Solid-State Circuits Conference Digest of Technical Paper*. IEEE, 2013.

[15] C. R. Doerr *et al*., "Single-chip silicon photonics 100-Gb/s coherent transceiver," *Optical Fiber Communication Conference*. Optical Society of America, 2014.

[16] K. Kang *et al.*, "On-chip coupled transmission line modeling for millimeter-wave applications using four-port measurements," *IEEE Trans. Adv. Packag.*, vol. 33, no. 1, pp. 153–159, Feb. 2010.

[17] R. Mongia *et al., RF and Microwave Coupled-Line Circuits*, 2nd ed., Norwood, MA, USA: Artech House, 2007, ch. 4, pp: 105–116.

[18] S. Kanazawa *et al*., "Ultra-compact 100 Gb transmitter optical sub-assembly for 40-km SMF transmission," *J. Lightw. Technol*., vol. 31, no. 4, pp: 602-608, 2013.

[19] W. Yao *et al*., "Experimental and numerical study of electrical crosstalk in photonic-integrated circuits," *J. Lightw. Technol.*, vol. 33, no. 4, pp: 934-942, 2015.

[20] X. Chen *et al*., "Characterization and digital pre-compensation of electro-optic crosstalk in silicon photonics I/Q modulators," European Conference on Optical Communications, 2016.

[21] L. Liao *et al*., "40 Gbit/s silicon optical modulator for high speed applications," *Electron. Lett*., vol. 43, no. 22, 2007.

[22] M. Streshinsky *et al*., "Highly linear silicon traveling wave Mach-Zehnder carrier depletion modulator based on differential drive," *Opt. Express*, vol. 21, no. 3, pp: 3818-3825, 2013.

[23] X. Tu *et al*., "Silicon optical modulator with shield coplanar waveguide electrodes," *Opt. Express*, vol. 22, no. 19, pp: 23724-23731, 2014.

[24] P. Dong *et al*., "High-speed low-voltage single-drive push-pull silicon Mach-Zehnder modulators," *Opt. Express*, vol. 20, no. 6, pp: 6163-6169, 2012.